ADV MATH SCI JOURNAL

Advances in Mathematics: Scientific Journal 8 (2019), no.3, 239–265
(Special issue on ICRAPAM)
ISSN 1857-8365 printed version
ISSN 1857-8438 electronic version

SEMI-ANALYTICAL SOLUTION FOR AMPEROMETRIC ENZYME ELECTRODE MODELLING WITH SUBSTRATE CYCLIC CONVERSION USING A NEW APPROACH TO HOMOTOPY PERTURBATION METHOD

S. Narmatha[1], *V. Ananthaswamy[2]

[1]Department of Mathematics, Lady Doak College, Madurai, Tamil Nadu, India

[2]PG & Research Department of Mathematics, The Madura College, Madurai, India

**Corresponding author E-mail: ananthu9777@rediffmail.com*

Abstract: The mathematical model pertaining to amperometric enzyme electrode with substrate cyclic conversion in a single enzyme membrane has been considered. The model is based on non-stationary diffusion equations containing a non-linear term related to Michaelis-Menten kinetics of the enzyme reaction. Semi-analytical solutions have been derived for the substrate concentration and reactant product concentrationin the steady state and the non-steady state using new approach to Homotopy perturbation method. The derived expressions are compared with the numerical results with the help of MATLAB and are found to be of excellent fit for experimental values of parameters. Analytical expressions for current are presented for steady state and non-steady state conditions. Further, the sensitivity of the parameters is also discussed.

Keywords: Biosensor; Amperometry; Michaelis – Menten kinetics; New approach to Homotopy perturbation method; Numerical Simulation; Sensitivity analysis.

1. Introduction

A biosensor is an analytical device, used for the detection of a chemical substance [3,4]. Biosensors consist of two components a biological entity that recognises the target analyte and the transducer that translates the biorecognition event into an electrical signal. The amperometric biosensors measure the changes of the current of a working indicator electrode by direct electrochemical oxidation or reduction of the products of the biochemical reaction[3]. In amperometric biosensors the potential of the electrode is held constant while the current is measured. The amperometric biosensors are known to be reliable, cheap and highly sensitive for environment, clinical and industrial purposes[1].

The goal of the investigation by RomasBaronas et al [1] was to make a model allowing computer simulation of the biosensors response utilising the amplification by conjugated electrochemical and enzymatic substrates conversion. The developed model was based on non stationary diffusion equations containing a nonlinear term related to the enzymatic reaction. The authors had carried out the digital simulation of the biosensor response using the implicit finite difference scheme.

We had derived the steady state and non-steady state analytical expressions for the substrate concentration and reactant product concentration using a new approach to Homotopy perturbation method. We had also derived the analytical expressions for current in the steady and non-steady state conditions.

2. Mathematical formulation of the problem

RomasBaronas et al [1] had considered biosensor as an enzyme electrode, containing a membrane with immobilised enzyme applied onto the surface of the electrochemical transducer. They considered the scheme of substrate (S)electrochemical conversion to a product (P) following catalysed with enzyme (E)product conversion to substrate:

$$S \rightarrow P \overset{E}{\rightarrow} S$$

Assuming the symmetrical geometry of the electrode and homogeneous distribution of immobilised enzyme in the enzyme membrane, the authors had framed the following governing nonlinear partial differential equations

$$\frac{\partial S}{\partial t} = D_S \frac{\partial^2 S}{\partial x^2} + \frac{V_{\max} P}{K_M + P}, \quad 0 < x < d,\ 0 < t \le T \tag{1}$$

$$\frac{\partial P}{\partial t} = D_P \frac{\partial^2 P}{\partial x^2} - \frac{V_{\max} P}{K_M + P}, \quad 0 < x < d,\ 0 < t \le T \tag{2}$$

where $x$is spatial coordinate, $t$is time, $S$is the substrate concentration, $P$is the reaction product concentration, $V_{\max}$ is the maximal enzymatic rate, K_M is the Michaelis constant, d is the enzyme layer thickness, D_S is the diffusion coefficient of the substrate, D_P is the diffusion coefficient of the product and T is the full time of operation.

$x = 0$represents the electrode surface, while $x = d$ represents the bulk solution/membrane surface. The operation of the biosensor starts when some of the substrate appears over the surface of the enzyme layer. Hence the initial conditions become

$$S(x,0) = 0,\ S(d,0) = S_0,\ 0 \le x < d \tag{3}$$

$$P(x,0) = 0,\ 0 \le x \le d \tag{4}$$

where S_0 is the concentration of the substrate in the bulk solution.

The boundary conditions are

$$S(0,t) = 0 \tag{5}$$

$$S(d,t) = S_0 \tag{6}$$

$$D_P \left(\frac{\partial P}{\partial x}\right)_{x=0} = -D_S \left(\frac{\partial S}{\partial x}\right)_{x=0} \tag{7}$$

$$P(d,t) = 0 \tag{8}$$

The current is measured as a response of the biosensor as follows

$$i(t) = n_e F D_S \left(\frac{\partial S}{\partial x}\right)_{x=0} = -n_e F D_P \left(\frac{\partial P}{\partial x}\right)_{x=0} \tag{9}$$

Where$n_e$is the number of electrons involved in a charge transfer at the electrode surface and $F$is Faraday constant. $F \approx 9.65 \times 10^4$ C/mol.

Eqns. (1) to (9) are converted to the dimensionless form using the following substitutions by Ismail et al [2]

$$S^* = \frac{S}{K_M},\ P^* = \frac{P}{K_M},\ x^* = \frac{x}{d},\ t^* = \frac{D_S t}{d^2},\ R = \frac{D_P}{D_S},\ i^*(t^*) = \frac{i(t)}{F V_{\max} d} \tag{10}$$

As per the experimental data, we observe that $D_P = D_S$, hence, hereafter, let us consider $D_P = D_S = D$

Define $\sigma^2 = \dfrac{V_{\max} d^2}{DK_M}$ (11)

Hence eqns. (1) to (9) in the dimensionless form become as follows

$$\frac{\partial S^*}{\partial t^*} = \frac{\partial^2 S^*}{\partial x^{*2}} + \sigma^2 \left(\frac{P^*}{1+P^*} \right) \tag{12}$$

$$\frac{\partial P^*}{\partial t^*} = \frac{\partial^2 P^*}{\partial x^{*2}} - \sigma^2 \left(\frac{P^*}{1+P^*} \right) \tag{13}$$

subject to the initial and boundary conditions

$$S^*(x^*,0) = 0,\ S^*(1,0) = S_0{}^* \tag{14}$$

$$P^*(x^*,0) = 0 \tag{15}$$

$$S^*(0,t^*) = 0 \tag{16}$$

$$S^*(1,t^*) = S_0{}^* \tag{17}$$

$$\left(\frac{\partial P^*}{\partial x^*} \right)_{x^*=0} = -\left(\frac{\partial S^*}{\partial x^*} \right)_{x^*=0} \tag{18}$$

$$P^*(1,t^*) = 0 \tag{19}$$

$$i^*(t^*) = \frac{n_e FD}{FV_{\max} d} \left(\frac{\partial S^*}{\partial x^*} \right)_{x^*=0} = -\frac{n_e FD}{FV_{\max} d} \left(\frac{\partial P^*}{\partial x^*} \right)_{x^*=0} \tag{20}$$

where $S_0{}^* = \dfrac{S_0}{K_M}$.

3. New approach to Homotopy perturbation method

Linear and non-linear differential equations can model many phenomena in different fields of Science and Engineering in order to present their behaviours and effects by mathematical concepts. Most of the non-linear differential equations do not have analytical solutions, but can be handled by semi-analytical or numerical methods. In order to obtain analytical solution of non-linear differential equations, semi-analytical methods such as the Variational Iteration method[11],Adomain decomposition method[12], Homotopy analysis method[13-16] andHomotopy perturbation method[19-24] are considered.

The Homotopy perturbation method is a powerful and efficient technique for finding solutions of nonlinear equations without the need of a linearization process.The method was first introduced by Hein1998 [5-10].HPM is a combination of the perturbation and homotopy methods. This method can take the advantages of the conventional perturbation method while eliminating its restrictions. In general, this method has been successfully applied to solve many kinds of linear and nonlinear equations in applied Sciences by many authors[25-36]. Lately, a new approach to HPM[17,18] is used to solve nonlinear differential equation in zeroth iteration.

4. Semi-analytical solution to the steady state of eqns. (12) to (19) and eqns. (1) to (8) usingnew approach to Homotopy perturbation method

Using new approach to HPM, the solution of eqns. (12) to (19) in steady state follows

$$S^* = S_0^* \left[1 - e^{-\sqrt{\frac{\sigma^2}{1+S_0^*}}x^*} + \frac{e^{-\sqrt{\frac{\sigma^2}{1+S_0^*}}} \sinh \sqrt{\frac{\sigma^2}{1+S_0^*}} x^*}{\sinh \sqrt{\frac{\sigma^2}{1+S_0^*}}} \right] \tag{21}$$

$$P^* = S_0^* \left[e^{-\sqrt{\frac{\sigma^2}{1+S_0^*}}x^*} - \frac{e^{-\sqrt{\frac{\sigma^2}{1+S_0^*}}} \sinh \sqrt{\frac{\sigma^2}{1+S_0^*}} x^*}{\sinh \sqrt{\frac{\sigma^2}{1+S_0^*}}} \right] \tag{22}$$

The solution of eqns. (1) to (8) in steady state follows

$$S = S_0 \left[1 - e^{-\sqrt{\frac{V_{\max}}{D(K_M+S_0)}}x} + \frac{e^{-\sqrt{\frac{V_{\max}d^2}{D(K_M+S_0)}}} \sinh \sqrt{\frac{V_{\max}}{D(K_M+S_0)}} x}{\sinh \sqrt{\frac{V_{\max}d^2}{D(K_M+S_0)}}} \right] \tag{23}$$

$$P = S_0 \left[e^{-\sqrt{\frac{V_{\max}}{D(K_M+S_0)}}x} - \frac{e^{-\sqrt{\frac{V_{\max}d^2}{D(K_M+S_0)}}} \sinh \sqrt{\frac{V_{\max}}{D(K_M+S_0)}} x}{\sinh \sqrt{\frac{V_{\max}d^2}{D(K_M+S_0)}}} \right] \tag{24}$$

5. Semi-analytical solution to eqns. (12) to (19) and eqns. (1) to (8) (non-steady state) using new approach to Homotopy perturbation method

Using new approach to HPM and Laplace transform technique [37,38], the solution to eqns.(12) to (19) in the non- steady state is evaluated as follows:

$$S^* = S_0^* \left(\begin{array}{l} 1 - e^{-\sqrt{\frac{\sigma^2}{1+S_0^*}}x^*} + \dfrac{e^{-\sqrt{\frac{\sigma^2}{1+S_0^*}}} \sinh \sqrt{\frac{\sigma^2}{1+S_0^*}} x^*}{\sinh \sqrt{\frac{\sigma^2}{1+S_0^*}}} + \sum_{n=0}^{\infty} 4(-1)^{n+1} \dfrac{\cos\left(\frac{2n+1}{2}\pi x^*\right) e^{-\left(\frac{(2n+1)^2}{4}\pi^2 t^*\right)}}{(2n+1)\pi} \\ + \sum_{n=1}^{\infty} \dfrac{2n\pi \sin(n\pi x^*) e^{-\left(\frac{\sigma^2}{1+S_0^*}+n^2\pi^2\right)t^*}}{\frac{\sigma^2}{1+S_0^*}+n^2\pi^2} \end{array} \right) \tag{25}$$

$$P^* = S_0^* \left(\left[e^{-\sqrt{\frac{\sigma^2}{1+S_0^*}}x^*} - \frac{e^{-\sqrt{\frac{\sigma^2}{1+S_0^*}}} \sinh \sqrt{\frac{\sigma^2}{1+S_0^*}} x^*}{\sinh \sqrt{\frac{\sigma^2}{1+S_0^*}}} \right] - \sum_{n=1}^{\infty} \frac{2n\pi \sin(n\pi x^*) e^{-\left(\frac{\sigma^2}{1+S_0^*}+n^2\pi^2\right)t^*}}{\frac{\sigma^2}{1+S_0^*}+n^2\pi^2} \right) \tag{26}$$

The solution of eqns. (1) to (8) in non steady state follows

$$S = S_0\left(\begin{array}{l} 1-e^{-\sqrt{\frac{V_{\max}}{D(K_M+S_0)}}x} + \dfrac{e^{-\sqrt{\frac{V_{\max}d^2}{D(K_M+S_0)}}}\sinh\sqrt{\dfrac{V_{\max}}{D(K_M+S_0)}}x}{\sinh\sqrt{\dfrac{V_{\max}d^2}{D(K_M+S_0)}}} + \sum_{n=0}^{\infty}4(-1)^{n+1}\dfrac{\cos\left(\dfrac{(2n+1)\pi x}{2d}\right)e^{-\left(\frac{(2n+1)^2\pi^2 Dt}{4d^2}\right)}}{(2n+1)\pi} \\ +\sum_{n=1}^{\infty}\dfrac{2n\pi\sin\left(\dfrac{n\pi x}{d}\right)e^{-\left(\frac{V_{\max}d^2}{D(K_M+S_0)}+n^2\pi^2\right)\frac{Dt}{d^2}}}{\dfrac{V_{\max}d^2}{D(K_M+S_0)}+n^2\pi^2} \end{array}\right) \tag{27}$$

$$P = S_0\left(\left[e^{-\sqrt{\frac{V_{\max}}{D(K_M+S_0)}}x} - \frac{e^{-\sqrt{\frac{V_{\max}d^2}{D(K_M+S_0)}}}\sinh\sqrt{\dfrac{V_{\max}}{D(K_M+S_0)}}x}{\sinh\sqrt{\dfrac{V_{\max}d^2}{D(K_M+S_0)}}}\right] - \sum_{n=1}^{\infty}\frac{2n\pi\sin\left(\dfrac{n\pi x}{d}\right)e^{-\left(\frac{V_{\max}d^2}{D(K_M+S_0)}+n^2\pi^2\right)\frac{Dt}{d^2}}}{\dfrac{V_{\max}d^2}{D(K_M+S_0)}+n^2\pi^2}\right) \tag{28}$$

We here note thatas $t \to \infty$, eqns. (25) to (28)exactly coincide with eqns. (21) and (24) respectively. This clearly indicates that the solution derived for the non-steady state converges to the solution derived for the steady state as $t \to \infty$.

6. Semi-analytical solution for current eqn. (20)

Substituting the non steady state solution of P^* in $i^*(t^*) = -\dfrac{n_e FD}{FV_{\max}d}\left(\dfrac{\partial P^*}{\partial x^*}\right)_{x^*=0}$, we get the non steady state current as follows

$$i^*(t^*) = \frac{n_e FDS_0{}^*}{FV_{\max}d}\left(\sqrt{\frac{\sigma^2}{1+S_0{}^*}}\left(1+\frac{e^{-\sqrt{\frac{\sigma^2}{1+S_0{}^*}}}}{\sinh\sqrt{\dfrac{\sigma^2}{1+S_0{}^*}}}\right) + \sum_{n=1}^{\infty}\frac{2n^2\pi^2 e^{-\left(\frac{\sigma^2}{1+S_0{}^*}+n^2\pi^2\right)t^*}}{\dfrac{\sigma^2}{1+S_0{}^*}+n^2\pi^2}\right) \tag{29}$$

and the steady state current as follows

$$i^*{}_\infty = \frac{n_e FDS_0{}^*}{FV_{\max}d}\sqrt{\frac{\sigma^2}{1+S_0{}^*}}\left(1+\frac{e^{-\sqrt{\frac{\sigma^2}{1+S_0{}^*}}}}{\sinh\sqrt{\dfrac{\sigma^2}{1+S_0{}^*}}}\right) \tag{30}$$

Using eqn. (10), the maximal biosensor current is given as follows

$$i_{\max} = i_\infty = \frac{n_e FDS_0}{K_M}\sqrt{\frac{V_{\max}d^2}{D(K_M+S_0)}}\left(1+\frac{e^{-\sqrt{\frac{V_{\max}d^2}{D(K_M+S_0)}}}}{\sinh\sqrt{\dfrac{V_{\max}d^2}{D(K_M+S_0)}}}\right) \tag{31}$$

7.Numerical simulation

The non-linear differential eqns. (12) and (13) with initial and boundary conditions given by eqns. (14) to (19) and the non-linear differential eqns. (1) and (2) with initial and boundary conditions given by eqns. (3) to (8) are also solved numerically. The function pdepe has been used in MATLAB software to solve the initial-boundary value problems numerically. The obtained analytical results are compared with the numerical simulation. The MATLAB program is given in Appendix D.

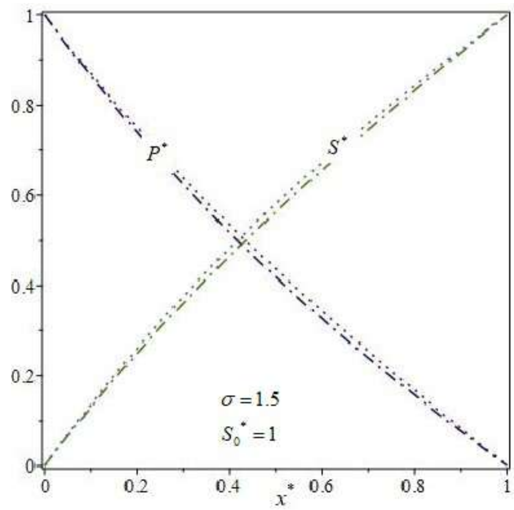

Fig1. The profile of the dimensionless substrate concentration(S^*) and reaction product concentration(P^*). The dotted lines represent the analytical solution and the lines with dots and dashes represent the numerical simulation.

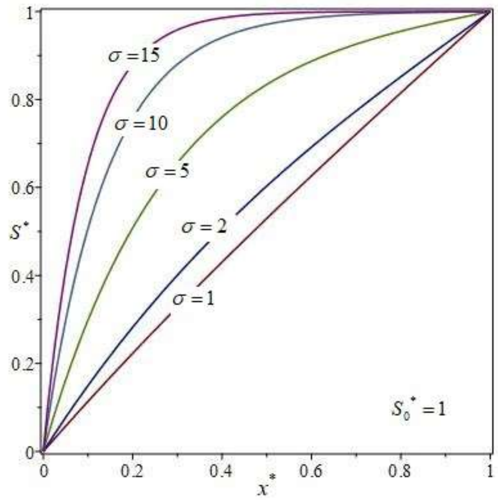

Fig2. The profile of the dimensionless substrate concentration(S^*) for various values of σ.

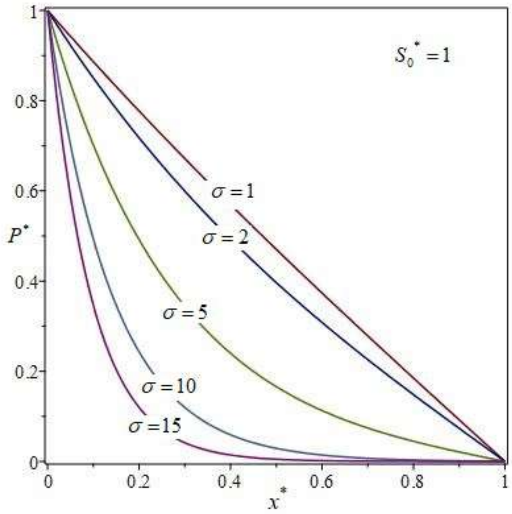

Fig3. The profile of the dimensionless reaction product concentration (P^*) for various values of σ.

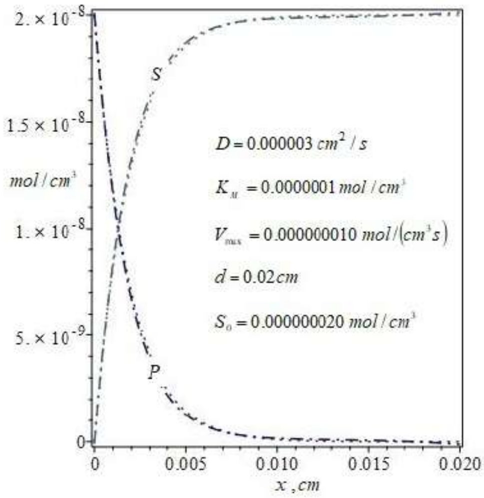

Fig4. The profile of the substrate concentration(S) and reaction product concentration(P). The dotted lines represent the analytical solution and the lines with dots and dashes represent the numerical simulation.

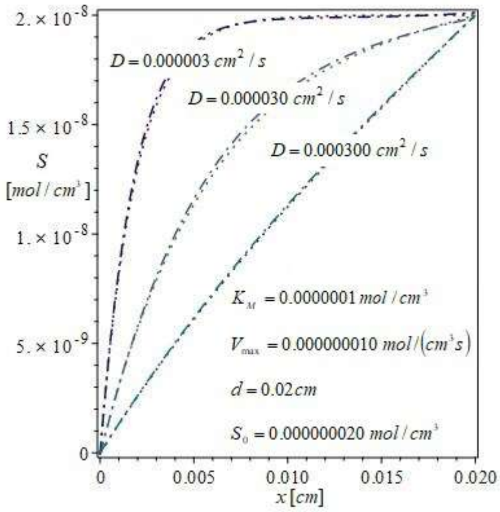

Fig5. The profile of the substrate concentration(S) versus spatial co-ordinate (x) for various values of D. The dotted lines represent the analytical solution and the lines with dots and dashes represent the numerical simulation.

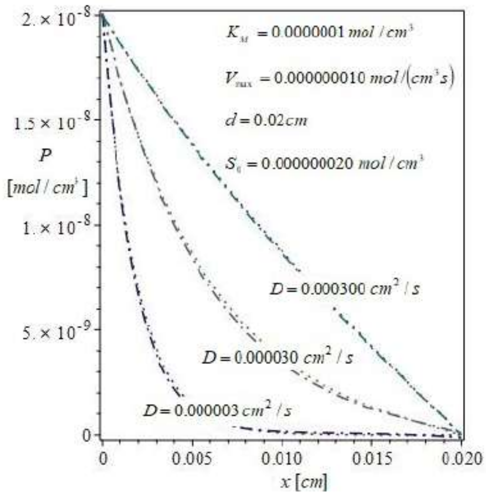

Fig6. The profile of the reaction product concentration(P) versus spatial co-ordinate (x) for various values of D. The dotted lines represent the analytical solution and the lines with dots and dashes represent the numerical simulation.

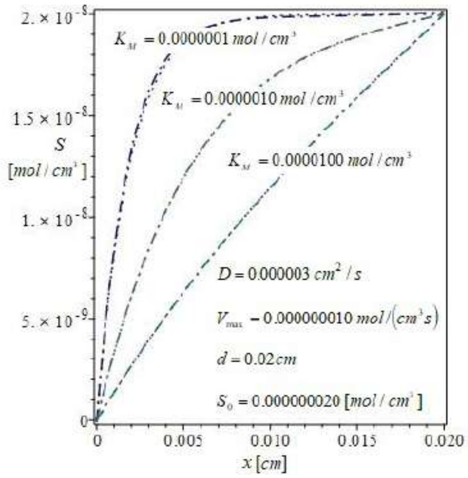

Fig7. The profile of the substrate concentration(S) versus spatial co-ordinate (x) for various values of K_M . The dotted lines represent the analytical solution and the lines with dots and dashes represent the numerical simulation.

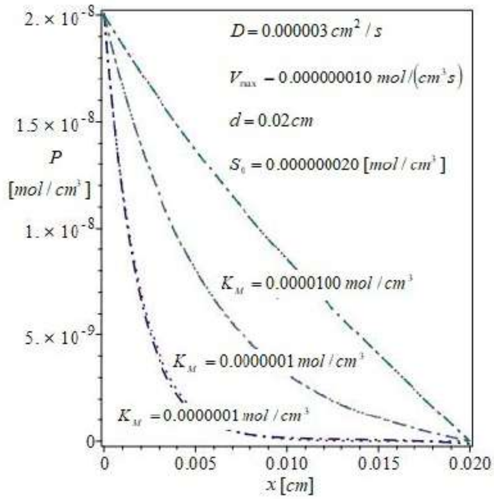

Fig8. The profile of the reaction product concentration(P) versus spatial co-ordinate (x) for various values of K_M . The dotted lines represent the analytical solution and the lines with dots and dashes represent the numerical simulation.

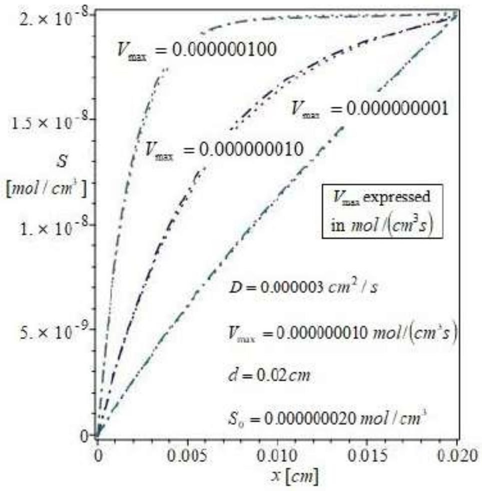

Fig9. The profile of the substrate concentration(S) versus spatial co-ordinate (x) for various values of $V_{\max}$. The dotted lines represent the analytical solution and the lines with dots and dashes represent the numerical simulation.

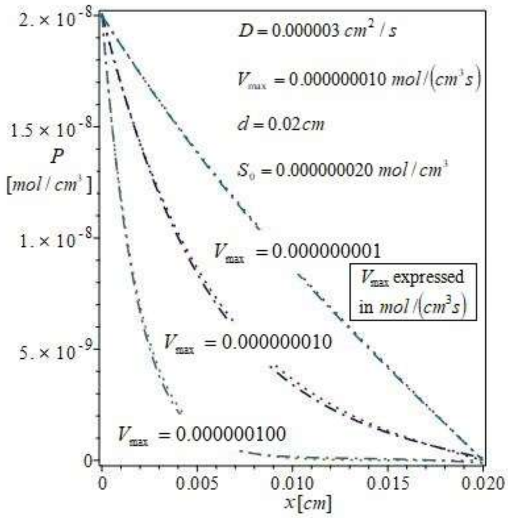

Fig10. The profile of the reaction product concentration(*P*) versus spatial co-ordinate (x) for various values of $V_{\max}$. The dotted lines represent the analytical solution and the lines with dots and dashes represent the numerical simulation.

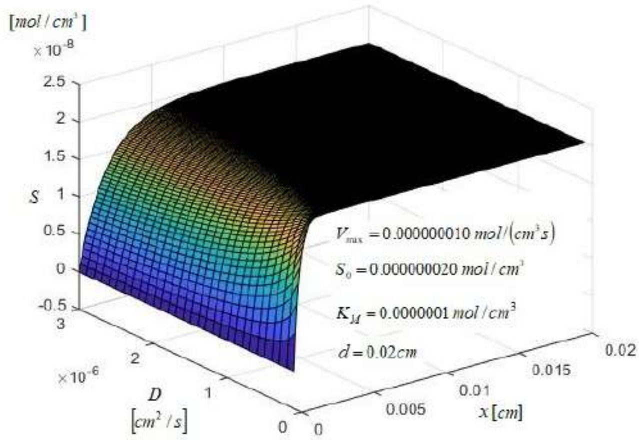

Fig11. Substrate concentration(S) versus spatial coordinate *x* and diffusion coefficient *D*.

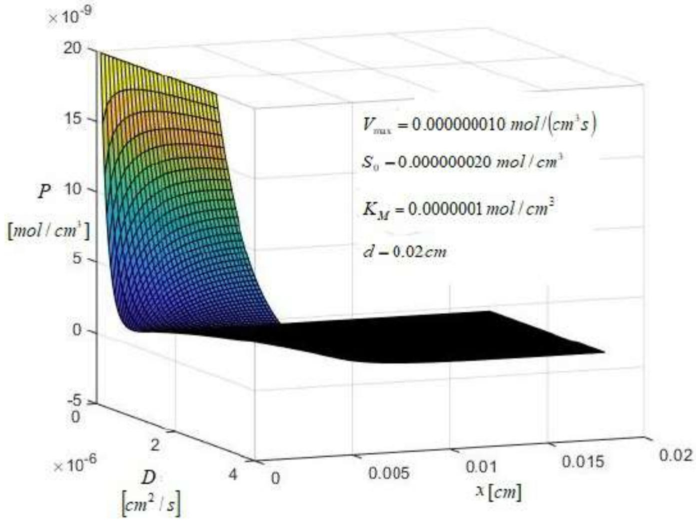

Fig12. Reaction product concentration(*P*) versus spatial coordinate *x* and diffusion coefficient *D*.

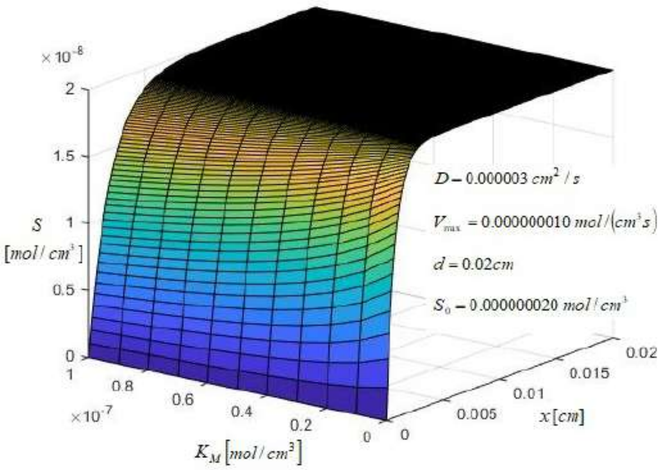

Fig13. Substrate concentration(S) versus spatial coordinate x and Michaelis constant K_M .

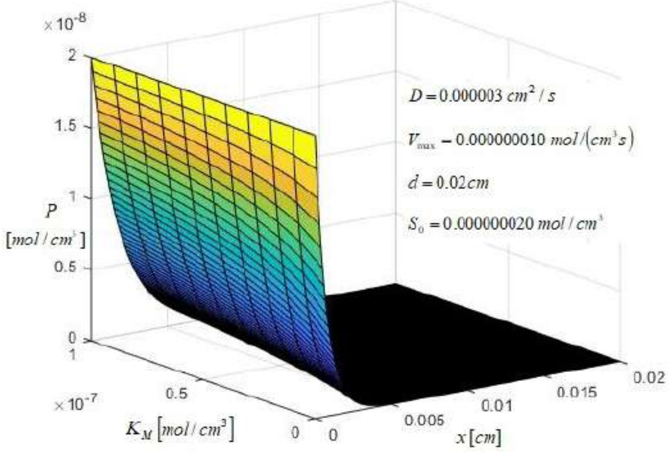

Fig14. Reaction product concentration(P) versus spatial coordinate x and Michaelis constant K_M .

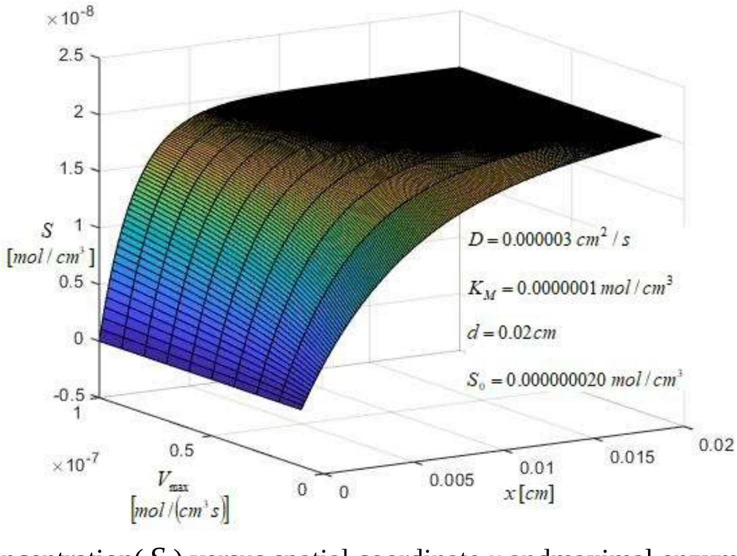

Fig15. Substrate concentration(S) versus spatial coordinate x andmaximal enzymatic rate V_{max} .

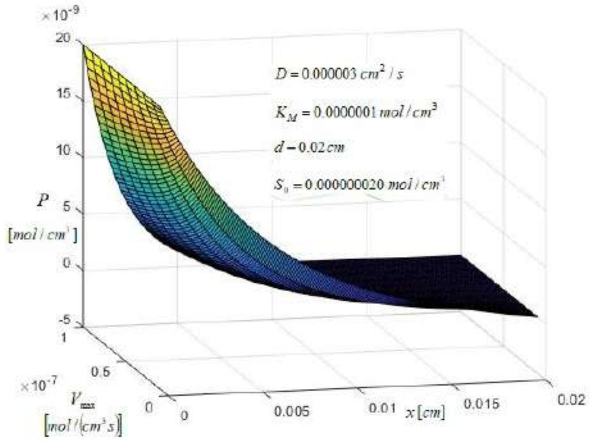

Fig16. Reaction product concentration(P) versus spatial coordinate x and maximal enzymatic rate $V_{\max}$.

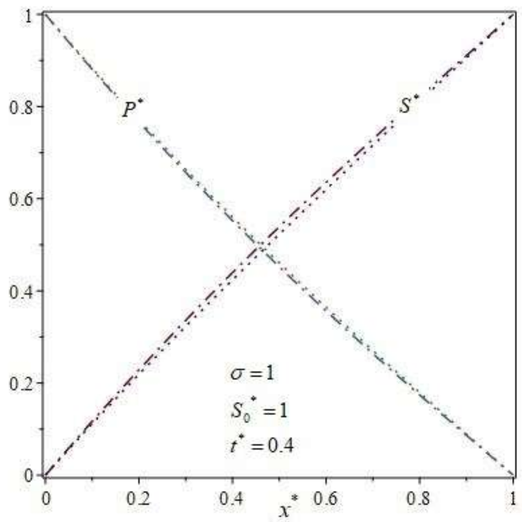

Fig17. Plot of dimensionless non steady state substrate concentration(S^*) and reaction product concentration(P^*)versus dimensionless spatial coordinate x^*. The dotted lines represent the analytical solution and the lines with dots and dashes represent the numerical simulation.

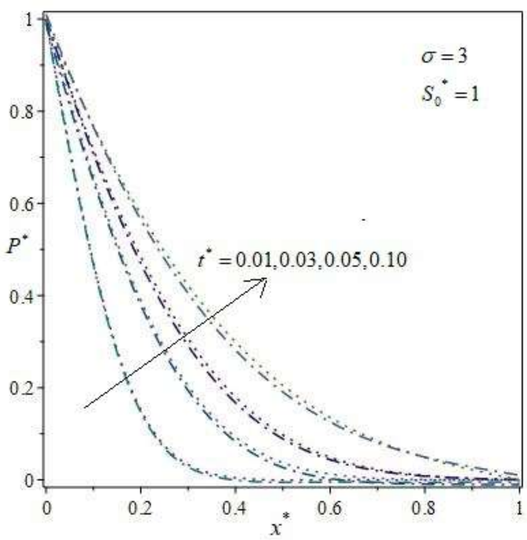

Fig18. Plot of dimensionless non steady state reaction product concentration (P^*) versus dimensionless spatial coordinate x^* for various values of t^* .The dotted lines represent the analytical solution and the lines with dots and dashes represent the numerical simulation.

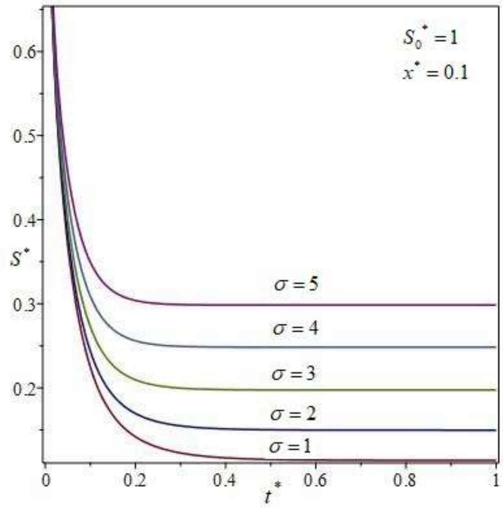

Fig19. Plot of dimensionless non steady state substrate concentration (S^*) versus dimensionless time t^* for various values of σ.

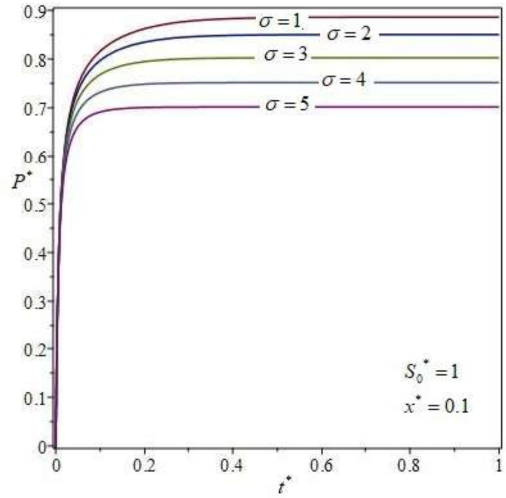

Fig20. Plot of dimensionless non steady state reaction product concentration(P^*)versus dimensionless time t^* for various values of σ.

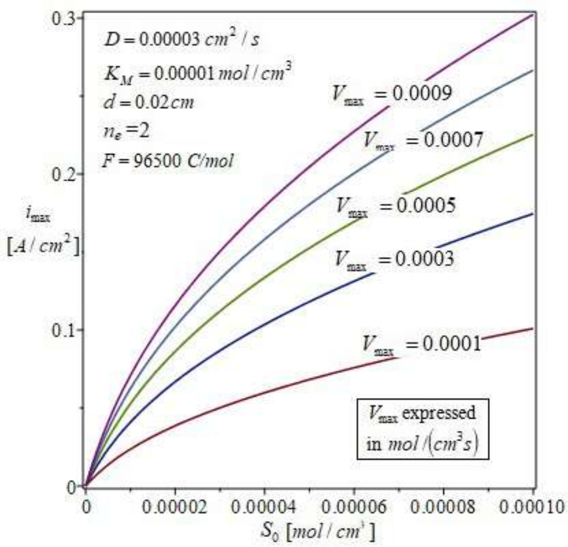

Fig21. The dependence of the maximal biosensor current i_{max} on S_0 for various values of V_{max}.

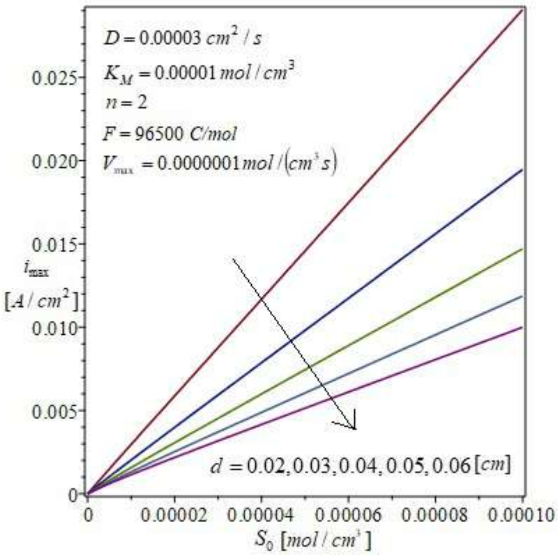

Fig22. The dependence of the maximal biosensor current $i_{\max}$ on S_0 for various values of d.

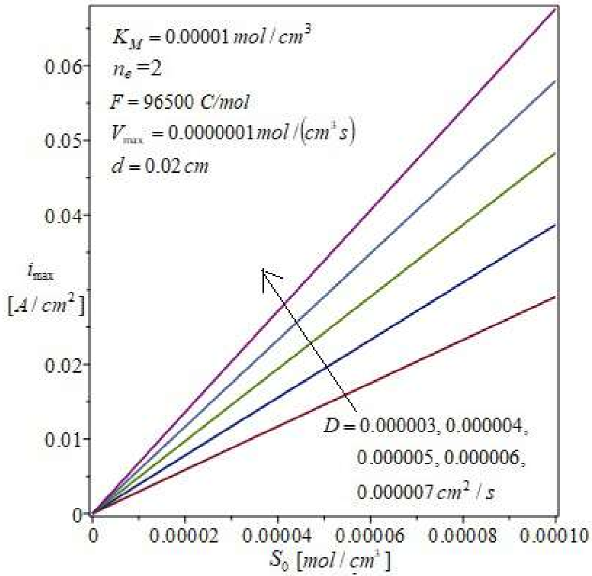

Fig23. The dependence of the maximal biosensor current $i_{\max}$ on S_0 for various values of D.

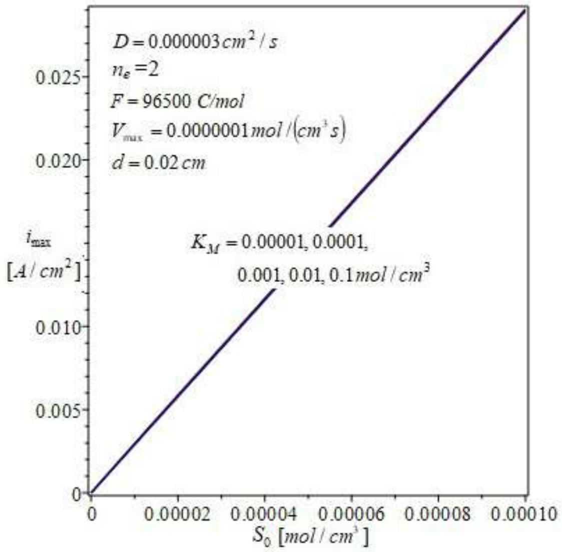

Fig24. The dependence of the maximal biosensor current $i_{\max}$ on S_0 for various values of K_M.

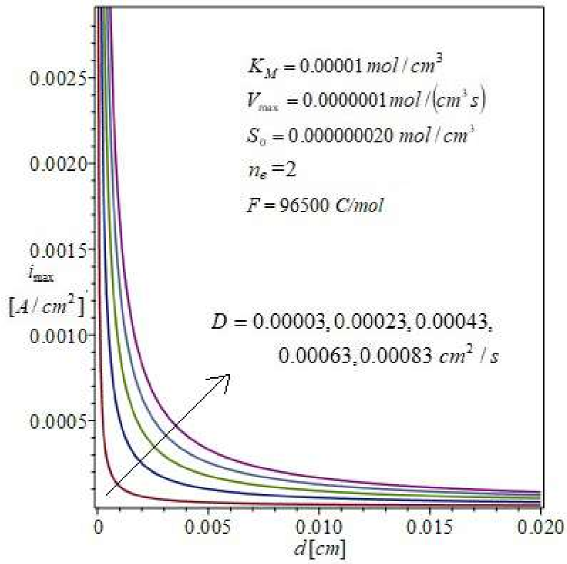

Fig25. The dependence of the maximal biosensor current $i_{\max}$ on d for various values of D.

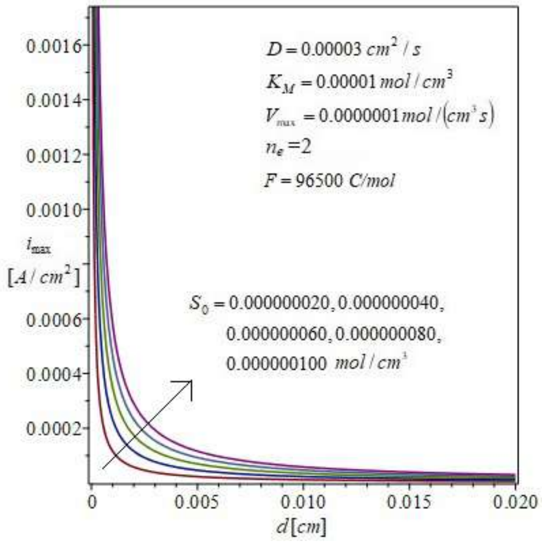

Fig 26. The dependence of the maximal biosensor current $i_{\max}$ on d for various values of S_0.

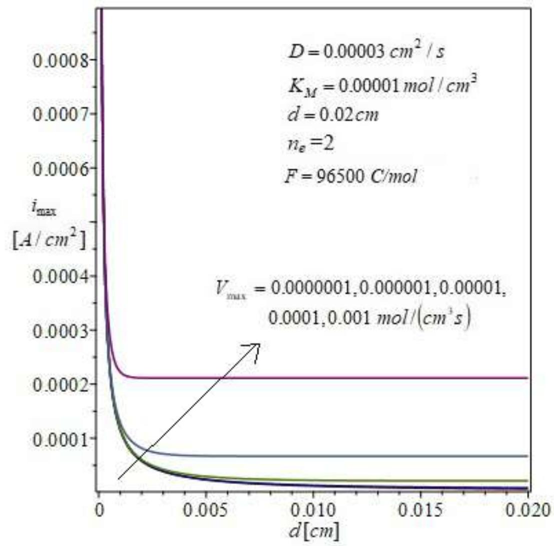

Fig 27. The dependence of the maximal biosensor current $i_{\max}$ on d for various values of $V_{\max}$.

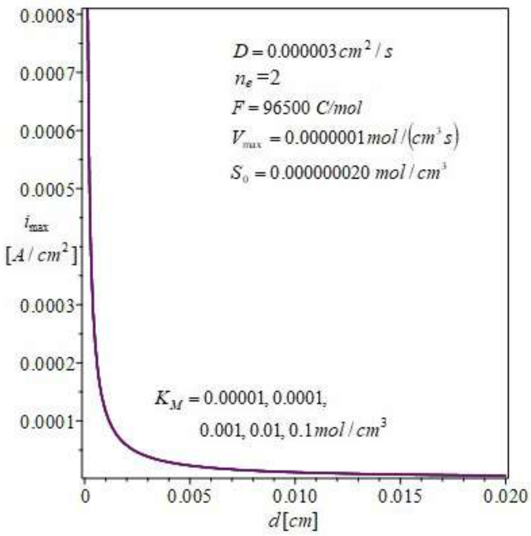

Fig 28. The dependence of the maximal biosensor current $i_{\max}$ on d for various values of K_M.

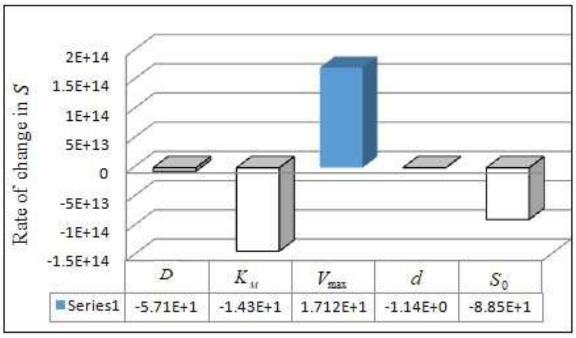

Fig 29. Sensitive analysis of parameters for *S.*

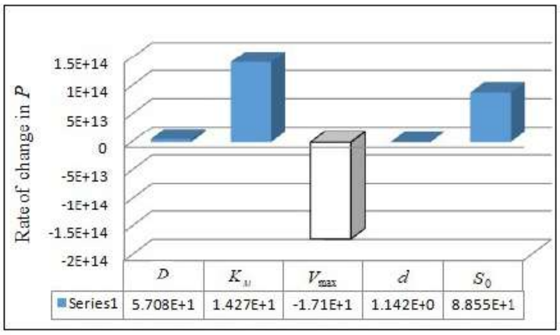

Fig30. Sensitive analysis of parameters for P.

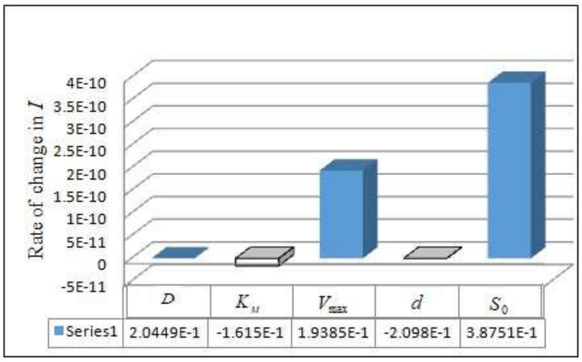

Fig31. Sensitive analysis of parameters for $i_{\max}$.

Table 1: Comparison between analytical values and numerical values in Fig. 1

$\sigma = 1.5,\ S_0^* = 1$				
	x^*	Numerical solution	Analytical solution	Absolute percentage error
P^*	0	1	1	0
	0.2	0.7398316080	0.7506387719	1.466
	0.4	0.5178647727	0.5351831490	3.34
	0.6	0.3265225987	0.3439012156	5.32
	0.8	0.1572218387	0.1681529572	6.95
	1	0	0	0
Average absolute percentage error				**2.85**
S^*	0	0	0	0
	0.2	0.2601305102	0.2493612285	4.14
	0.4	0.4820711959	0.4648168510	3.58
	0.6	0.6734062126	0.6560987844	2.57
	0.8	0.8427188243	0.8318470425	1.29
	1	1	1	0
Average absolute percentage error				**1.93**

Table 2: Comparison between analytical values and numerical values in Fig. 17

$\sigma = 1,\ S_0^* = 1,\ t^* = 0.4$				
	x^*	Numerical solution	Analytical solution	Absolute percentage error
P^*	0	1	1	0
	0.2	.7664803607	.7713196686	0.63
	0.4	.5525067020	.5603604244	1.42
	0.6	.3563129966	.3642991454	2.24
	0.8	.1741361958	.1792099059	2.91
	1	0	0	0
Average absolute percentage error				**1.20**
S^*	0	0	0	0
	0.2	.2287153054	.2189629008	4.26
	0.4	.4396212556	.4239368673	3.57
	0.6	.6356443302	.6201222897	2.44
	0.8	.8207419226	.8112821227	1.15
	1	1	1	0
Average absolute percentage error				**1.90**

Table 3: Comparison between analytical values and numerical values in Fig. 18

$\sigma = 3,\ S_0^* = 1$					
	t^*	x^*	Numerical solution	Analytical solution	Absolute percentage error
P^*	0.10	0	1	1	0
		0.2	.5645282694	.5770063790	2.21
		0.4	.2816910527	.2992320250	6.22
		0.6	.1255576406	.1351773082	7.66
		0.8	0.049454271	0.04840812589	2.12
		1	0	0	0

	Average absolute percentage error	**3.04**

8. Results and discussion

The steady state (Appendix A) and the non-steady state (Appendix B) analytical expressions for the substrate concentration and reactant product concentration have been derived. The semi-analytical steady state solutions for dimensionless substrate concentration $\left(S^*\right)$and dimensionless reactant product concentration$\left(P^*\right)$are compared with the numerical solutions derived using Matlab in Fig1. The semi-analytical steady state solutions for the substrate concentration(S) and reactant product concentration(P) are compared with the numerical solutions derived using Matlab for various values of parameters in Figs3 to 10. The semi-analytical non steady state solutionsfor the dimensionless substrate concentration$\left(S^*\right)$ and dimensionless reactant product concentration$\left(P^*\right)$are compared with the numerical solutions derived using Matlab in Figs. 17 and18. Tables 1 to 3 show that the maximum deviation between the semi-analytical and numerical values is a maximum of 3%. This shows that the semi-analytical solutions make an excellent fit with the numerical solutions for experimental values of parameters [1].

Fig2. represents the dimensionless substrate concentration (S^*) versus dimensionless spatial coordinate (x^*) for different values of parameter σ. Fig3. represents the dimensionless reactant product concentration (P^*) versus dimensionless spatial coordinate (x^*) for different values of parameter σ. Fig19 represents the dimensionless substrate concentration (S^*) versus dimensionless time (t^*) for different values of parameter σ. Fig20. represents the dimensionless reactant product concentration (P^*) versus dimensionless time (t^*) for different values of parameter σ. From the figures, it is clear to observe that the value of S^* increases with increase in σ, while the value of P^* decreases with increase in σ.

From Figs. 5, 7 and 9, we observe that the substrate concentration (S) decreases with increase in D, decreases with increase in K_M and increases with increase in $V_{\max}$. From Figs. 6, 8 and 10, we observe that the reactant product concentration (P) increases with increase in D, increases with increase in K_M and decreases with increase in $V_{\max}$.

Figs. 11, 13 and 15 show the substrate concentration (S) versus spatial co-ordinate x and D, K_M and $V_{\max}$. respectively. Figs. 12, 14 and 16 show the reactant product concentration (P) versus spatial co-ordinate x and D, K_M and $V_{\max}$ respectively.

Figs. 21 to 24 show the variation of steady state current $i_{\max}$ with respect to S_0 for various values of $V_{\max}$, *d*, D and K_M respectively. Figs. 25 to 28 show the variation of steady state current $i_{\max}$ with respect to *d* for various values of D, S_0, $V_{\max}$ and K_M respectively. From the figures it is clear that $i_{\max}$ increases with increase in S_0, while it decreases with increase in *d.*

Differential sensitivity analysis is based on partial differentiation of the aggregated model. We have found the partial derivative of substrate concentration (S), reactant product concentration (P) and steady state current $i_{\max}$ (dependent variables) with respect to the parameters D, K_M, $V_{\max}$, d and S_0 (independent variables). For the experimental values of parameters, numerical value of rate of change of S, P and $i_{\max}$ are obtained and the sensitivity analysis of the parameters is given in Figs. 29 to 31.

From Fig29.it is inferred that $V_{\max}$ has positive impact on substrate concentration (S) while *D,* K_M, d and S_0 have negative impact on the same. K_M accounts for the maximum negative impact on S.From Fig30.it is obvious that D, K_M, d and S_0 have positive impact on reactant product concentration (P) while $V_{\max}$ has negative impact. K_M accounts for the maximum positive impact on P.From Fig31.it is inferred that D, $V_{\max}$ and S_0 have positive impact on steady state current $i_{\max}$ while K_M, d have negative impact on the same . S_0 accounts for the maximum positive impact on $i_{\max}$ .Next to the parameter S_0, the parameter $V_{\max}$ has more positive impact on current.

From Figs 19 and 20 , we infer that S^* reaches its steady state after $t^* = 0.6$ and P^* reaches its steady state after $t^* = 0.5$.

9. Conclusion

In this paper, steady state and time dependent approximate analytical expressions for thesubstrate concentration and reactant product concentration are reported. The new Homotopy perturbation method is used to obtain the solution. Our results are of excellent fit with the numerical results. Analytical expressions for current are also presented for steady and non-steady state conditions. The obtained semi-analytical results under non-steady state will help the researchers to interpret the effect of the different parameters over the substrate concentration, product concentration and steady state current.

Appendix A

Semi-analytical solution for the steady state model of eqns.(12) to (19) and eqns. (1) to (8)

Eqns. (12) and (13) in steady state become

$$\frac{\partial^2 S^*}{\partial x^{*2}} + \sigma^2\left(\frac{P^*}{1+P^*}\right) = 0 \tag{A.1}$$

$$\frac{\partial^2 P^*}{\partial x^{*2}} - \sigma^2\left(\frac{P^*}{1+P^*}\right) = 0 \tag{A.2}$$

subject to the boundary conditions

$$S^*(0,t^*) = 0 \tag{A.3}$$

$$S^*(1,t^*) = S_0{}^* \tag{A.4}$$

$$\left(\frac{\partial P^*}{\partial x^*}\right)_{x^*=0} = -\left(\frac{\partial S^*}{\partial x^*}\right)_{x^*=0} \tag{A.5}$$

$$P^*(1,t^*) = 0 \tag{A.6}$$

To solve eqns. (A.1) and (A.2), we introduce a new function $G^* = S^* + P^*$, so, that eqns (A.1) and (A.2) together give

$$\frac{\partial^2 G^*}{\partial x^{*2}} = 0 \tag{A.7}$$

subject to the boundary conditions

$$\left(\frac{\partial G^*}{\partial x^*}\right)_{x^*=0} = 0 \tag{A.8}$$

$$G^*(1,t^*) = S_0{}^* \tag{A.9}$$

Solving eqns. (A.7) to (A.9), we get

$$G^* = S_0{}^* \tag{A.10}$$

We construct the homotopy for eqn. (A.2) as follows

$$(1-p)\left[\frac{\partial^2 P^*}{\partial x^{*2}} - \sigma^2\left(\frac{P^*}{1+S_0{}^*}\right)\right] + p\left[\frac{\partial^2 P^*}{\partial x^{*2}} - \sigma^2\left(\frac{P^*}{1+P^*}\right)\right] = 0 \tag{A.11}$$

Let the approximate solution of (A.2) be

$$P^* = P_0{}^* + P_1{}^* p + P_2{}^* p^2 + \dots \tag{A.12}$$

Substituting eqn. (A.12) in eqn. (A.11) and equating the coefficients of p^0, we get

$$\frac{\partial^2 P_0^*}{\partial x^{*2}} - \sigma^2 \left(\frac{P_0^*}{1+S_0^*} \right) = 0 \tag{A.13}$$

Let $k = \dfrac{\sigma^2}{1+S_0^*}$, so that the above equation becomes

$$\frac{\partial^2 P_0^*}{\partial x^{*2}} - kP_0^* = 0 \tag{A.14}$$

Solving eqn. (A.13) using its boundary conditions, we get

$$P_0^* = S_0^* \left[e^{-\sqrt{k}x^*} - \frac{e^{-\sqrt{k}} \sinh \sqrt{k} x^*}{\sinh \sqrt{k}} \right] \tag{A.15}$$

From eqn. (A.12), we have $P^* \approx P_0^*$, hence we get

$$P^* \approx S_0^* \left[e^{-\sqrt{k}x^*} - \frac{e^{-\sqrt{k}} \sinh \sqrt{k} x^*}{\sinh \sqrt{k}} \right] \tag{A.16}$$

Since $G^* = S^* + P^*$, we get

$$S^* = G^* - P^* = S_0^* \left[1 - e^{-\sqrt{k}x^*} + \frac{e^{-\sqrt{k}} \sinh \sqrt{k} x^*}{\sinh \sqrt{k}} \right] \tag{A.17}$$

Hence the solution for eqns. (12) to (19) is as follows

$$S^* = S_0^* \left[1 - e^{-\sqrt{\frac{\sigma^2}{1+S_0^*}}x^*} + \frac{e^{-\sqrt{\frac{\sigma^2}{1+S_0^*}}} \sinh \sqrt{\frac{\sigma^2}{1+S_0^*}} x^*}{\sinh \sqrt{\frac{\sigma^2}{1+S_0^*}}} \right] \tag{A.18}$$

$$P^* = S_0^* \left[e^{-\sqrt{\frac{\sigma^2}{1+S_0^*}}x^*} - \frac{e^{-\sqrt{\frac{\sigma^2}{1+S_0^*}}} \sinh \sqrt{\frac{\sigma^2}{1+S_0^*}} x^*}{\sinh \sqrt{\frac{\sigma^2}{1+S_0^*}}} \right] \tag{A.19}$$

Substituting eqns. (10) and (11) in (A.18) and (A.19) , we get the semi-analytical solution for the steady state model of equations (1) to (8) as follows

$$S = S_0 \left[1 - e^{-\sqrt{\frac{V_{\max}}{D(K_M+S_0)}}x} + \frac{e^{-\sqrt{\frac{V_{\max} d^2}{D(K_M+S_0)}}} \sinh \sqrt{\frac{V_{\max}}{D(K_M+S_0)}} x}{\sinh \sqrt{\frac{V_{\max} d^2}{D(K_M+S_0)}}} \right] \tag{A.20}$$

$$P = S_0 \left[e^{-\sqrt{\frac{V_{\max}}{D(K_M+S_0)}}x} - \frac{e^{-\sqrt{\frac{V_{\max} d^2}{D(K_M+S_0)}}} \sinh \sqrt{\frac{V_{\max}}{D(K_M+S_0)}} x}{\sinh \sqrt{\frac{V_{\max} d^2}{D(K_M+S_0)}}} \right] \tag{A.21}$$

Appendix B

Semi-analytical solution for eqns.(12) to (19) and eqns. (1) to (8)

To solve eqns. (12) to (19), we introduce a new function $H^* = S^* + P^*$, so that eqns. (12) and (13) together give

$$\frac{\partial H^*}{\partial t^*} = \frac{\partial^2 H^*}{\partial x^{*2}} \tag{B.1}$$

subject to the initial and boundary conditions

$$H^*(x^*, 0) = 0 \tag{B.2}$$

$$\left(\frac{\partial H^*}{\partial x^*}\right)_{x^*=0} = 0 \tag{B.3}$$

$$H^*(1, t^*) = S_0^* \tag{B.4}$$

Applying Laplace transform to eqns. (B.1) to (B.4), we get

$$\frac{\partial \overline{H^*}}{\partial t^*} - \frac{\partial^2 \overline{H^*}}{\partial x^{*2}} = 0 \tag{B.5}$$

subject to the initial and boundary conditions

$$t^* = 0,\ \overline{H^*} = 0 \tag{B.6}$$

$$x^* = 0,\ \frac{\partial \overline{H^*}}{\partial x^*} = 0 \tag{B.7}$$

$$x^* = 1,\ \overline{H^*} = \frac{S_0^*}{s} \tag{B.8}$$

Solving eqns. (B.5) to (B.8), we get

$$\overline{H^*} = \frac{S_0^* \cosh \sqrt{s} x^*}{s \cosh \sqrt{s}} \tag{B.9}$$

Now, let us invert eqn.(B.9) using the complex inversion formula.

If $\overline{y}(s)$ represents the Laplace transform of a function $y(\tau)$, then according to the complex inversion formula $y(\tau) = \frac{1}{2\pi i} \oint_C \exp(s\tau) \overline{y}(s) ds$ where the integration has to be performed along a line $s = c$ in the complex plane where $s = x + iy$. The real number c is chosen in such a way that $s = c$ lies to the right of all the singularities, but is otherwise assumed to be arbitrary. In practice, the integral is evaluated by considering the contour integral presented on the right-hand side of the equation, which is then evaluated using the so-called Bromwich contour. The contour integral is then evaluated using the residue theorem.

In order to invert eqn.(B.9), we need to evaluate $\operatorname{Re} s \left(\frac{S_0^* \cosh \sqrt{s} x^*}{s \cosh \sqrt{s}} \right)$.

Now, finding the poles of $\overline{H^*}$ we see that there is a pole at $s = 0$ and there are infinitely many poles given by the solution of the equation $\cosh\left(\sqrt{s}\right) = 0$

(ie) there are infinite number of poles at $s_n = -(2n+1)^2 \frac{\pi^2}{4}$, where $n = 1, 2, 3, ...$

Hence, we note that

$$L^{-1}(\overline{H^*}) = \operatorname{Re} s \left[e^{st} \left(\frac{S_0^* \cosh \sqrt{s} x^*}{s \cosh \sqrt{s}} \right) \right]_{s=0} + \operatorname{Re} s \left[e^{st} \left(\frac{S_0^* \cosh \sqrt{s} x^*}{s \cosh \sqrt{s}} \right) \right]_{s=s_n} \tag{B.10}$$

The first residue in eqn. (B.10) is given by

$$\operatorname{Re}s\left[e^{st}\left(\frac{S_0^{\ *}\cosh\sqrt{s}x^*}{s\cosh\sqrt{s}}\right)\right]_{s=0}$$

$$=\begin{matrix} lt \\ s\to 0\end{matrix}\; s\, e^{st}\, \frac{S_0^{\ *}\cosh\sqrt{s}x^*}{s\cosh\sqrt{s}}$$

$$=S_0^{\ *} \tag{B.11}$$

The second residue in eqn. (B.10) is given by

$$\operatorname{Re}s\left[e^{st}\left(\frac{S_0^{\ *}\cosh\sqrt{s}x^*}{s\cosh\sqrt{s}}\right)\right]_{s=s_n}$$

$$=S_0^{\ *}\begin{matrix} lt \\ s\to s_n\end{matrix}\; e^{st}\, \frac{\cosh\sqrt{s}x^*}{s\frac{d}{ds}\left(\cosh\sqrt{s}\right)}$$

$$=\sum_{n=0}^{\infty}4(-1)^{n+1}S_0^{\ *}\,\frac{\cos\left(\frac{2n+1}{2}\pi x^*\right)e^{-\left(\frac{(2n+1)^2}{4}\pi^2t^*\right)}}{(2n+1)\pi} \tag{B.12}$$

Using eqns. (B.11) and (B.12) in eqn.(B.10), we get

$$H^*=S_0^{\ *}+\sum_{n=0}^{\infty}4(-1)^{n+1}S_0\,\frac{\cos\left(\frac{2n+1}{2}\pi x^*\right)e^{-\left(\frac{(2n+1)^2}{4}\pi^2t^*\right)}}{(2n+1)\pi}$$

$$=S_0^{\ *}\left(1+\sum_{n=0}^{\infty}4(-1)^{n+1}\,\frac{\cos\left(\frac{2n+1}{2}\pi x^*\right)e^{-\left(\frac{(2n+1)^2}{4}\pi^2t^*\right)}}{(2n+1)\pi}\right) \tag{B.13}$$

To solve for P^*, we construct the homotopy for eqn. (13) as follows

$$(1-p)\left[\frac{\partial P^*}{\partial t^*}-\frac{\partial^2P^*}{\partial x^{*2}}+\sigma^2\left(\frac{P^*}{1+S_0^{\ *}}\right)\right]+p\left[\frac{\partial P^*}{\partial t^*}-\frac{\partial^2P^*}{\partial x^{*2}}+\sigma^2\left(\frac{P^*}{1+P^*}\right)\right]=0 \tag{B.14}$$

Let the approximate solution of eqn.(13) be

$$P^*=P_0^{\ *}+P_1^{\ *}p+P_2^{\ *}p^2+\cdots \tag{B.15}$$

Substituting eqn. (B.15) in eqn. (B.14) and equating the coefficients of p^0, we get

$$\frac{\partial P_0^{\ *}}{\partial t^*}=\frac{\partial^2P_0^{\ *}}{\partial x^{*2}}-\sigma^2\left(\frac{P_0^{\ *}}{1+S_0^{\ *}}\right) \tag{B.16}$$

Let $k=\dfrac{\sigma^2}{1+S_0^{\ *}}$, so that eqn (B.16) becomes

$$\frac{\partial P_0^{\ *}}{\partial t^*}=\frac{\partial^2P_0^{\ *}}{\partial x^{*2}}-kP_0^{\ *} \tag{B.17}$$

Applying Laplace transform to eqn. (B.17) and to its boundary conditions, we get

$$\frac{\partial\overline{P_0^{\ *}}}{\partial t^*}=\frac{\partial^2\overline{P_0^{\ *}}}{\partial x^{*2}}-k\overline{P_0^{\ *}} \tag{B.18}$$

subject to the following initial and boundary conditions

$$t^*=0,\ \overline{P_0^{\ *}}=0 \tag{B.19}$$

$$x^* = 0,\ \overline{P_0^*} = \frac{S_0^*}{s} \tag{B.20}$$

$$x^* = 1,\ \overline{P_0^*} = 0 \tag{B.21}$$

Solving eqns. (B.18) to (B.21), we get

$$\overline{P_0^*} = \frac{S_0^*}{s}\left[e^{-\sqrt{s+k}x^*} - \frac{e^{-\sqrt{s+k}}\sinh\sqrt{s+k}x^*}{\sinh\sqrt{s+k}}\right] \tag{B.22}$$

In order to invert eqn.(B.22), we need to use the complex inversion formula, which means we need to evaluate $\operatorname{Re}s\left(\frac{S_0^*}{s}\left[e^{-\sqrt{s+k}x^*} - \frac{e^{-\sqrt{s+k}}\sinh\sqrt{s+k}x^*}{\sinh\sqrt{s+k}}\right]\right)$.

Now, finding the poles of $\overline{P_0^*}$, we see that there is a pole at $s = 0$ and there are infinitely many poles given by the solution of the equation $\sinh\sqrt{s+k} = 0$

(ie) there are infinite number of poles at $s_n = -k - n^2\pi^2$, where $n = 1, 2, 3, ...$

Hence, we note that

$$L^{-1}\left(\overline{P_0^*}\right) = \operatorname{Re}s\left[e^{st}\left(\frac{S_0^*}{s}\left[e^{-\sqrt{s+k}x^*} - \frac{e^{-\sqrt{s+k}}\sinh\sqrt{s+k}x^*}{\sinh\sqrt{s+k}}\right]\right)\right]_{s=0}$$

$$+\operatorname{Re}s\left[e^{st}\left(\frac{S_0^*}{s}\left[e^{-\sqrt{s+k}x^*} - \frac{e^{-\sqrt{s+k}}\sinh\sqrt{s+k}x^*}{\sinh\sqrt{s+k}}\right]\right)\right]_{s=s_n} \tag{B.23}$$

The first residue in eqn. (B.23) is given by

$$\operatorname{Re}s\left[e^{st}\left(\frac{S_0^*}{s}\left[e^{-\sqrt{s+k}x^*} - \frac{e^{-\sqrt{s+k}}\sinh\sqrt{s+k}x^*}{\sinh\sqrt{s+k}}\right]\right)\right]_{s=0}$$

$$= \underset{s\to 0}{lt}\, s\,e^{st}\left(\frac{S_0^*}{s}\left[e^{-\sqrt{s+k}x^*} - \frac{e^{-\sqrt{s+k}}\sinh\sqrt{s+k}x^*}{\sinh\sqrt{s+k}}\right]\right)$$

$$= \left(S_0^*\left[e^{-\sqrt{k}x^*} - \frac{e^{-\sqrt{k}}\sinh\sqrt{k}x^*}{\sinh\sqrt{k}}\right]\right) \tag{B.24}$$

The second residue in eqn. (B.23) is given by

$$\operatorname{Re}s\left[e^{st}\left(\frac{S_0^*}{s}\left[e^{-\sqrt{s+k}x^*} - \frac{e^{-\sqrt{s+k}}\sinh\sqrt{s+k}x^*}{\sinh\sqrt{s+k}}\right]\right)\right]_{s=s_n}$$

$$= -\underset{s\to s_n}{lt}\ S_0^* e^{st}\frac{e^{-\sqrt{s+k}}\sinh\sqrt{s+k}x^*}{s\frac{d}{ds}\left(\sinh\sqrt{s+k}\right)}$$

$$= -S_0^*\sum_{n=1}^{\infty}\frac{2n\pi\sin(n\pi x^*)e^{-\left(k+n^2\pi^2\right)t^*}}{k+n^2\pi^2} \tag{B.25}$$

Using eqns. (B.24) and (B.25) in eqn.(B.23), we get

$$P_0^* = \left(S_0^*\left[e^{-\sqrt{k}x^*} - \frac{e^{-\sqrt{k}}\sinh\sqrt{k}x^*}{\sinh\sqrt{k}}\right]\right) - S_0^*\sum_{n=1}^{\infty}\frac{2n\pi\sin(n\pi x^*)e^{-\left(k+n^2\pi^2\right)t^*}}{k+n^2\pi^2}$$

$$= S_0^*\left(\left[e^{-\sqrt{k}x^*} - \frac{e^{-\sqrt{k}}\sinh\sqrt{k}x^*}{\sinh\sqrt{k}}\right] - \sum_{n=1}^{\infty}\frac{2n\pi\sin(n\pi x^*)e^{-\left(k+n^2\pi^2\right)t^*}}{k+n^2\pi^2}\right)$$

From eqn. (B.15), we get

$$P^* \approx P_0^* = S_0^*\left(\left[e^{-\sqrt{k}x^*} - \frac{e^{-\sqrt{k}}\sinh\sqrt{k}x^*}{\sinh\sqrt{k}}\right] - \sum_{n=1}^{\infty}\frac{2n\pi\sin(n\pi x^*)e^{-\left(k+n^2\pi^2\right)t^*}}{k+n^2\pi^2}\right) \tag{B.26}$$

Since $H^* = S^* + P^*$, we get

$$S^* = H^* - P^* = S_0^*\left(1 + \sum_{n=0}^{\infty}4(-1)^{n+1}\frac{\cos\left(\frac{2n+1}{2}\pi x^*\right)e^{-\left(\frac{(2n+1)^2}{4}\pi^2 t^*\right)}}{(2n+1)\pi}\right)$$

$$-S_0^*\left(\left[e^{-\sqrt{k}x^*} - \frac{e^{-\sqrt{k}}\sinh\sqrt{k}x^*}{\sinh\sqrt{k}}\right] - \sum_{n=1}^{\infty}\frac{2n\pi\sin(n\pi x^*)e^{-\left(k+n^2\pi^2\right)t^*}}{k+n^2\pi^2}\right)$$

$$= S_0^*\left(\begin{array}{l} 1 - e^{-\sqrt{k}x^*} + \dfrac{e^{-\sqrt{k}}\sinh\sqrt{k}x^*}{\sinh\sqrt{k}} + \displaystyle\sum_{n=0}^{\infty}4(-1)^{n+1}\frac{\cos\left(\frac{2n+1}{2}\pi x^*\right)e^{-\left(\frac{(2n+1)^2}{4}\pi^2 t^*\right)}}{(2n+1)\pi} \\ + \displaystyle\sum_{n=1}^{\infty}\frac{2n\pi\sin(n\pi x^*)e^{-\left(k+n^2\pi^2\right)t^*}}{k+n^2\pi^2} \end{array}\right) \tag{B.27}$$

Hence the solution for eqns. (12) to (19) is as follows

$$S^* = S_0^*\left(\begin{array}{l} 1 - e^{-\sqrt{\frac{\sigma^2}{1+S_0^*}}x^*} + \dfrac{e^{-\sqrt{\frac{\sigma^2}{1+S_0^*}}}\sinh\sqrt{\dfrac{\sigma^2}{1+S_0^*}}x^*}{\sinh\sqrt{\dfrac{\sigma^2}{1+S_0^*}}} + \displaystyle\sum_{n=0}^{\infty}4(-1)^{n+1}\frac{\cos\left(\frac{2n+1}{2}\pi x^*\right)e^{-\left(\frac{(2n+1)^2}{4}\pi^2 t^*\right)}}{(2n+1)\pi} \\ + \displaystyle\sum_{n=1}^{\infty}\frac{2n\pi\sin(n\pi x^*)e^{-\left(\frac{\sigma^2}{1+S_0^*}+n^2\pi^2\right)t^*}}{\dfrac{\sigma^2}{1+S_0^*}+n^2\pi^2} \end{array}\right) \tag{B.28}$$

$$P^* = S_0^*\left(\left[e^{-\sqrt{\frac{\sigma^2}{1+S_0^*}}x^*} - \frac{e^{-\sqrt{\frac{\sigma^2}{1+S_0^*}}}\sinh\sqrt{\dfrac{\sigma^2}{1+S_0^*}}x^*}{\sinh\sqrt{\dfrac{\sigma^2}{1+S_0^*}}}\right] - \sum_{n=1}^{\infty}\frac{2n\pi\sin(n\pi x^*)e^{-\left(\frac{\sigma^2}{1+S_0^*}+n^2\pi^2\right)t^*}}{\dfrac{\sigma^2}{1+S_0^*}+n^2\pi^2}\right) \tag{B.29}$$

Substituting eqns. (10) and (11) in (B.28) and (B.29) , we get the solution for equations (1) to (8) as follows.

$$S=S_0\left(1-e^{-\sqrt{\frac{V_{\max}}{D(K_M+S_0)}}x}+\frac{e^{-\sqrt{\frac{V_{\max}d^2}{D(K_M+S_0)}}}\sinh\sqrt{\frac{V_{\max}}{D(K_M+S_0)}}x}{\sinh\sqrt{\frac{V_{\max}d^2}{D(K_M+S_0)}}}+\sum_{n=0}^{\infty}4(-1)^{n+1}\frac{\cos\left(\frac{(2n+1)\pi x}{2d}\right)e^{-\left(\frac{(2n+1)^2\pi^2Dt}{4d^2}\right)}}{(2n+1)\pi}\right.$$
$$\left.+\sum_{n=1}^{\infty}\frac{2n\pi\sin\left(\frac{n\pi x}{d}\right)e^{-\left(\frac{V_{\max}d^2}{D(K_M+S_0)}+n^2\pi^2\right)\frac{Dt}{d^2}}}{\frac{V_{\max}d^2}{D(K_M+S_0)}+n^2\pi^2}\right) \tag{B.30}$$

$$P=S_0\left(\left[e^{-\sqrt{\frac{V_{\max}}{D(K_M+S_0)}}x}-\frac{e^{-\sqrt{\frac{V_{\max}d^2}{D(K_M+S_0)}}}\sinh\sqrt{\frac{V_{\max}}{D(K_M+S_0)}}x}{\sinh\sqrt{\frac{V_{\max}d^2}{D(K_M+S_0)}}}\right]-\sum_{n=1}^{\infty}\frac{2n\pi\sin\left(\frac{n\pi x}{d}\right)e^{-\left(\frac{V_{\max}d^2}{D(K_M+S_0)}+n^2\pi^2\right)\frac{Dt}{d^2}}}{\frac{V_{\max}d^2}{D(K_M+S_0)}+n^2\pi^2}\right) \tag{B.31}$$

Appendix: C
Nomenclature

Symbols	Meaning
x	spatial coordinate in cm
t	time in s
S	substrate concentration in mol/cm^3
P	reaction product concentration in mol/cm^3
$V_{\max}$	maximal enzymatic rate in mol/(cm^{3}s)
K_M	Michaelis constant in mol/cm^3
d	enzyme layer thickness in cm
D_S	diffusion coefficient of the substrate in cm^2/s
D_P	diffusion coefficient of the product in cm^2/s
T	full time of operation in s
$i(t)$	density of current at time t in A/cm^2
n_e	number of electrons involved in a charge transfer at the electrode surface
F	Faraday constant, $F\approx 9.65*10^4$ C/mol
$i_{\max}$	steady state current i_∞ in A/cm^2
S^*	dimensionless substrate concentration
P^*	dimensionless reaction product concentration
σ^2	Damkohler number (Da)
x^*	dimensionless spatial coordinate
t^*	dimensionless time

Appendix: D
MATLAB program to find the numerical solution of eqns. (12)-(19)

```
Function pdepe
m = 0;
x = linspace(0,1);
t = linspace(0,0.1);
```

```
sol = pdepe(m,@pdex4pde,@pdex4ic,@pdex4bc,x,t);
u1 = sol(:,:,1);
u2 = sol(:,:,2);
figure
plot(x,u1(end,:))
title('u1(x,t)')
xlabel('Distance x')
ylabel('u1(x,2)')
%-----------------------------------------------------------------
figure
plot(x,u2(end,:))
title('u2(x,t)')
xlabel('Distance x')
ylabel('u2(x,2)')
% --------------------------------------------------------------
function [c,f,s] = pdex4pde(x,t,u,DuDx)
c = [1; 1];
f = [1; 1] .* DuDx;
si=1;
F=-(si^2*u(2))/((1+u(2)));
s=[-F; F];
% --------------------------------------------------------------
function u0 = pdex4ic(x);
u0 = [0;0];
% --------------------------------------------------------------
function [pl,ql,pr,qr] = pdex4bc(xl,ul,xr,ur,t)
pl = [ul(1)-0;ul(2)-1];
ql = [0;0];
pr = [ur(1)-1;ur(2)-0];
qr = [0;0];
```

MATLAB program to find the numerical solution of eqns. (1)-(8)

```
functionpdepe
m = 0;
x = linspace(0,0.020);
t = linspace(0,100000);
sol = pdepe(m,@pdex4pde,@pdex4ic,@pdex4bc,x,t);
u1 = sol(:,:,1);
u2 = sol(:,:,2);
figure
plot(x,u1(end,:))
title('u1(x,t)')
xlabel('Distance x')
ylabel('u1(x,2)')
%-----------------------------------------------------------------
figure
plot(x,u2(end,:))
title('u2(x,t)')
xlabel('Distance x')
ylabel('u2(x,2)')
% --------------------------------------------------------------
function [c,f,s] = pdex4pde(x,t,u,DuDx)
c = [1; 1];
f = [1; 1] .* DuDx;
d=0.000003;
```

```
k=0.0000100;
v=0.000000100;
F=-(v*u(2))/((k+u(2))*d);
s=[-F; F];
% ----------------------------------------------------------
function u0 = pdex4ic(x);
u0 = [0;0.000000020];
% ----------------------------------------------------------
function [pl,ql,pr,qr] = pdex4bc(xl,ul,xr,ur,t)
pl = [ul(1)-0;ul(2)-0.000000020];
ql = [0;0];
pr = [ur(1)-0.000000020;ur(2)-0];
qr = [0;0];
```

References

[1] RomasBaronas, JuozasKulys, FeliksasIvanauskas,Modellingamperometric enzyme electrode with substrate cyclic conversion,Biosensors and Bioelectronics,Volume 19, Issue 8, 2004, Pages 915-922

[2] I. Ismail, G. Oluleye , IJ Oluwafemi , et al. Mathematical modelling of an enzyme-based biosensor, Int J BiosenBioelectron, 2017;3(2):265–268.

[3] Turner, Anthony; Wilson, George; Kaube, Isao ,Biosensors:Fundamentals and Applications, Oxford, UK: Oxford University Press, 1987, p. 770.

[4] Bănică, Florinel-Gabriel , Chemical Sensors and Biosensors:Fundamentals and Applications. Chichester, UK: John Wiley & Sons, 2012, p. 576.

[5] J. H. He, Homotopy perturbation method a new nonlinear analytical technique. Applied Mathematics and Computations, 2003, pp. 135 :73- 79.

[6] J. H. He, Homotopy perturbation technique, Compt. Method, Appl. Mech. Eng. 178, 1999, pp. 257-262.

[7] J. H. He, A simple perturbation approach to Blasius equation, Applied Mathematics and Computations, 2003, pp 140: 217-222.

[8] J. H. He, Some asymptotic methods for strongly non-linear equations, International of modern Physics, 2006, pp: B. 20: 1141- 1199.

[9] J. H. He, G C Wu, F Austin F, The variational iteration method which should be followed, Non-linear Science Letters, 2010, pp: A 1, 1- 30.

[10] J. H. He, A Coupling method of a Homotopy technique and perturbation technique for non- linear problems, International Journal of Non-linear Mechanics, 2000, pp: 35: 37-43.

[11] A.M. Wazwaz, Thevariational iteration method for solving linear and nonlinear ODEs and scientific models with variable coefficients, Central European Journal of Engineering, 2014,Vol.4, pp. 64–71.

[12] P. Felicia Shirly, S. Narmatha and L. Rajendran, Analytical solution of nonlinear dynamics of a self-igniting reaction diffusion system using modified Adomian decomposition method, Int. J. Chem. Engg., 2014, 825797.

[13] V. Ananthaswamy, S. Kala And L. Rajendran Approximate Analytical Solution Of Non-Linear Initial Value Problem For An Autocatalysis In A Continuous Stirred Tank Reactor: Homotopy Analysis Method, International Journal Of Mathematical Archive- 5(4), 2014

[14] V. Ananthaswamy , Sp. Ganesan And L. Rajendran, Approximate Analytical Solution Of Non-Linear Reaction-Diffusion Equation In Microwave Heating Model In A Slab: Homotopy Analysis Method

[15] M. Subha, V. Ananthaswamy, L. Rajendran , A Comment On Liao's Homotopy Analysis Method Int. Journal Of Applied Sciences And Engineering Research, Vol. 3, Issue 1, 2014

[16] V. Ananthaswamy, L. SahayaAmalraj Thermal Stability Analysis Of Reactive Hydromagnetic Third-Gradefluid Using Homotopy Analysis Method, International Journal Of Modern Mathematical Sciences, 2016, 14(1): 25-41

[17] V.Ananthaswamy, S.Narmatha, Comparison between the new Homotopy perturbation method and modified Adomain decomposition method in solving a system of non-linear self igniting

reaction diffusion equations**,** International Journal of Emerging Technologies and Innovative Research (www.jetir.org), ISSN:2349-5162, Vol.6, Issue 5, page no.51-59, May-2019
[18] P. Felicia Shirly, S. Narmatha, L. Rajendran, Analytical solution of boundary value problem in reactive gas absorption,International Journal of Mathematical Archive-4(6), 2013, 228-242
[19] D. Shanthi, V. Ananthaswamy, L. Rajendran, Analysis of non-linear reaction-diffusion processes with Michaelis-Menten kinetics by a new Homotopy perturbation method, Natural Science 5 (09), 2014, 1034.
[20] V. Ananthaswamy, R. Shanthakumari, M. Subha, Simple analytical expressions of the non-linear reaction diffusion process in an immobilized biocatalyst particle using the new homotopy perturbation method, review of bioinformatics and biometrics, 2014, pp: 3, 22-28.
[21] V. Ananthaswamy , C. Thangapandi , J. Joy Brieghti , MuthuramalingamRasi&RajendranLakshmanan, Analytical expression of nonlinear partial differential equations in mediated electrochemical induction of chemical reaction, Advances in Chemical Science, 2015, 4. 7. 10.14355/sepacs.2015.04.002.
[22] V. Ananthaswamy&L. Rajendran, Approximate Analytical Solution of Non-Linear Kinetic Equation in a Porous Pellet, Global Journal of Pure and Applied Mathematics, 2012
[23] V. Ananthaswamy& L. Rajendran, Analytical Solution of Non-Isothermal Diffusion-Reaction Processes and Effectiveness Factors, ISRN Physical Chemistry, 2013, 10.1155/2013/487240
[24] V. Ananthaswamy& L. Rajendran, Analytical Solutions of Some Two-Point Non-Linear Elliptic Boundary Value Problems, Applied Mathematics,2012, 03. 1044-1058. 10.4236/am.2012.39154.
[25] J. Biazar, F. Badpeima, F. Azimi, Application of the homotopy perturbation method to Zakharov–Kuznetsov equations, Computers & Mathematics with Applications,Volume 58, Issues 11–12,2009,Pages 2391-2394
[26] R.M. Devi, O.M. Kirthiga, and L Rajendran, Analytical Expression for the Concentration of Substrate and Product in Immobilized Enzyme System in Biofuel/Biosensor, Applied Mathematics, 2015, 6, 1148-1160
[27] M. M .Mousa, S. F. Ragab, Nturfosch, Application of the Homotopy perturbation method to linear and nonlinear schrodinger equations, zeitschrift fur naturforschung, 2008, pp:63:140-144.
[28] M. Rasi, L. Rajendran, and A. Subbiah, Analytical expression of transient current-potential for redox enzymatic homogenous system, Sen. Actuat. B. Chem., B208, 2015, pp. 128-136.
[29] M. Rasi, L. Rajendran and M. V. Sankaranarayanan, Transient current expression for oxygen transport in composite mediated biocathodes, J. Elec. Chem. **Soc.**, 162 (9), 2015, pp. H671-H680.
[30] L. Rajendran, S. Anitha, Reply to Comments on analytical solution of amperometric enzymatic reactions based on HPM, Electrochim. Acta 102, 2013, pp. 474-476.
[31] N.Mehala,L.Rajendran, Analysis of Mathematical modeling on potentiometric Biosensors, ISRN Biochemistry, 2014, pp.1-11.
[32] S. Anitha, A. Subbiah, L. Rajendran, Analytical expression of non-steady –state concentrations and current pertaining to compounds present in the enzyme membrane of Biosensor, The Journal of Physical chemistry, 115(17), 2011, pp.4299- 4306.
[33] S. Ganesan, S. Anitha, A. Subbiah, L. Rajendran, Mathematical modeling of a carrier-mediated transport process in a liquid membrane, J. Membr. Biol. 246, 2013, 435–442.
[34] A. Meena, L. Rajendran, Mathematical modeling of amperometric and potentiometric biosensors and system of nonlinear equations-Homotopy perturbation approach, J. Electroanal. Chem. 644 , 2010, 50–59.
[35] A. Eswari, L. Rajendran, Analytical expressions pertaining to the concentrations of catechol, -quinone and current at PPO-modified micro-cylinder biosensor for diffusion kinetic model, J. Electroanal. Chem. 660 ,2011, 200–208.
[36] K. Venugobal, A. Eswari, L. Rajendran, Mathematical model for steady state current at PPO-modified micro-cylinder biosensors, J. Biomed. Sci. Eng. 4, 2011, 631–641.
[37] Kara Asher, An introduction to Laplace transform, international journal of science and research, 2013, 2(1), pp.601-606.
[38] Zhiqiang Zhou and XuemeiGao, Laplace transform methods for a free boundary problem of time-fractional partial differential equation system, Hindawi Discrete Dynamics in Nature and Society, Vol.2017, 2017, pp. 1-9.